

Balancing Control of a Self-driving Bicycle

T. J. Yeh, Hao-Tien Lu and Po-Hsuan Tseng

Department of Power Mechanical Engineering, National Tsing Hua University, Hsinchu 30013, Taiwan

Keywords: Balancing Control, Bicycle, Convex Combination, Linear Matrix Inequality.

Abstract: In this research, a self-driving bicycle is constructed and the balancing control using the handlebar is studied. The controller is designed based on a model which characterizes the bicycle's lateral dynamics under speed variations. As the model can be decomposed into a convex combination of four linear subsystems with time-varying coefficients, the proposed controller also consists of a convex combination of four linear, full-state feedback controllers. It is proved that if the full-state feedback controllers satisfy a set of linear matrix inequalities, the bicycle can maintain its lateral stability regardless of speed changes. Both simulations and experiments verify that the proposed controller can achieve robust balancing performance under various operating conditions.

1 INTRODUCTION

As the least expensive means of wheeled transportation, bicycles are widely used for many activities such as commute, sport, recreation and so on. Bicycles are considered to be environmentally friendly because they can reduce the traffic congestion and air pollution in urban areas. The recent introduction of electric bicycles can further enhance the range and mobility of bicycles. From system dynamics perspective, bicycles are in the category of wheeled-inverted-pendulum vehicles and exhibit interesting dynamic behavior. Modeling, analysis, and control of bicycles thus have attracted significant attention in research community ever since they were invented.

Whipple(Whipple, 1899) pioneered his work on bicycle modeling by firstly deriving the equations of motion of the bicycle. His model, which considered the bicycle as an assembly of four rigid bodies, is both rigorous and complete. However, it is not suitable for control system studies because it is highly nonlinear and complex. For this reason, several simplified models have been proposed. For example, Sharp(Sharp, 1971) used a four-degree-of-freedom model to analyze the forward stability of a bicycle. Lowell et.al.(Lowell and McKel, 1982) lumped the whole bicycle as a point mass and used an inverted pendulum to describe the lateral dynamics. K. J. Astrom(Astrom et al., 2005) further augmented the inverted pendulum model by incorporating steering angle as the input to the front fork assembly. In (Meijaard et al., 2007), a benchmark model for the bi-

cycle was presented by Meijaard et. al.. This model, which is a linear time-varying system parameterized by the bicycle speed, is obtained by linearizing the motion equations for small perturbations around the constant-speed straight-ahead upright trajectory.

Regarding the control studies for bicycles, the recent advances in digital computers, sensor and actuator technologies have drawn significant research interests on developing self-balancing bicycles. For instance, Beznos et al.(Beznos et al., 1998) controlled the precession of the gyroscopes to generate a gyroscopic torque to counteract the destabilizing gravitational torque so as to balance a bicycle. In (Cerone et al., 2010), the authors exploited the linear-parameter-varying (LPV) nature of the bicycle model proposed in (Meijaard et al., 2007) to design a control system that automatically balances a riderless bicycle in the upright position. Their control problem is formulated as the design of an LPV state-feedback controller that guarantees stability when the speed varies within a given range and its derivative is bounded. While the steering torque is treated as the control input in (Cerone et al., 2010), Tanaka and Murakami(Tanaka and Murakami, 2004) applied PD control to modulate the steering angle to stabilize the roll motion of the bicycle. In (Huang et al., 2017), the authors developed a miniaturized humanoid robot to ride and pedal a bicycle of comparable size. The robot balances and steers the bicycle via controlling the angle of the handlebar. The controller, which is designed based-on a constant-speed bicycle model, can automatically counteract the mass imbalance in the

robot-bicycle system and allow it to perform straight-line steering and cornering.

In this research, balancing control of a real-size, self-driving bicycle is studied. The model adopted here for controller design considers speed variations and thus can be characterized as an LPV system as in (Meijaard et al., 2007). However, in stead of solving a infinite family of linear matrix inequalities (LMI's) as in the reference, the model is converted into a special format so that only a small number of LMI needed to be solved to devise the controller for robust performance under speed variations. The paper is organized as follows: A model that describes the speed-dependent lateral dynamics of the bicycle is given in Section II. Section III shows how the dynamic model can be converted into a tractable form so as to conduct robust balancing control design against speed variations. The performance of the control system is verified numerically in Section IV. Section V describes the hardware setup of the self-driving bicycle and performs experimental validation on the control performance. Finally, conclusions are given in Section VI.

2 MODELING OF THE LATERAL DYNAMICS

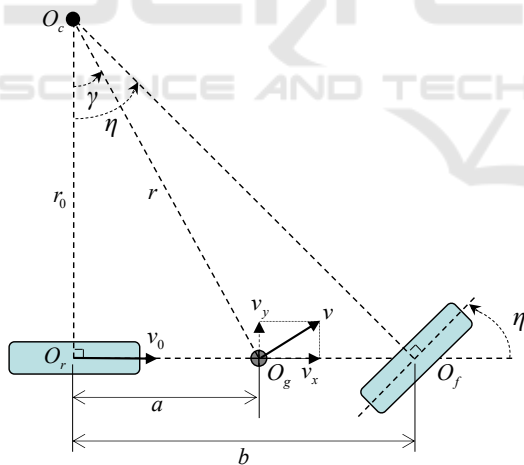


Figure 1: Top view of a bicycle.

This section derives a model that describes the lateral dynamics of a bicycle. The modeling approach here is adopted from (Huang et al., 2017). To begin with, the kinematic relations among crucial motion variables are analyzed.

2.1 Kinematic Analysis

Fig. 1 shows the top view of a bicycle in which O_g is the center of gravity (COG) of the bicycle, O_f is the

center of the front wheel, and O_r is the center of the rear wheel. Assume that the rear wheel is driven with speed v_0 and the front wheel is steered with a directional angle η . Driving and steering actions make the bicycle turn with respect to an instantaneous center of rotation O_c . Under the no-slip condition, O_c is the intersection of the two extension lines respectively from the axles of the front and rear wheels. Let $a = \overline{O_r O_g}$, $b = \overline{O_f O_g}$, $r_0 = \overline{O_c O_r}$, $r = \overline{O_c O_g}$, and $\gamma = \angle O_r O_c O_g$, so the following trigonometric relations hold:

$$r = \frac{a}{\sin \gamma}, \quad (1)$$

and

$$r_0 = \frac{a}{\tan \gamma} = \frac{b}{\tan \eta}. \quad (2)$$

Notice that the yaw rate of the bicycle, which is denoted by $\dot{\phi}$, is equal to $\frac{v_0}{r_0}$. From the second equality in (2), $\dot{\phi}$ can be written as

$$\dot{\phi} = \frac{\tan \eta}{b} v_0. \quad (3)$$

Let v be the magnitude of the bicycle's velocity at the COG O_g , and v_x and v_y be the components of the velocity along and perpendicular to the bicycle body. Since the bicycle body is rigid, we have $v_x = v_0$, and v and v_y are related to v_0 respectively by

$$v = r \dot{\phi} = \frac{a \tan \eta}{b \sin \gamma} v_0, \quad (4)$$

and

$$v_y = v \sin \gamma = \frac{a \tan \eta}{b} v_0. \quad (5)$$

2.2 Dynamic Analysis

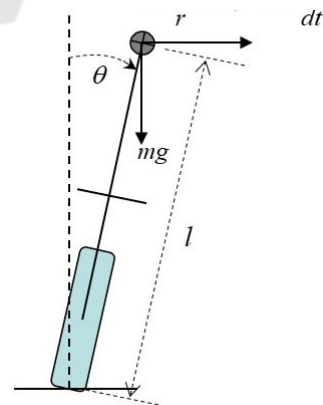


Figure 2: Frontal view of a bicycle.

In the the frontal view shown in Fig. 2, the bicycle is modeled as an inverted pendulum whose mass m is concentrated at the COG. The COG is located at

a distance of l from the ground contact point with a roll angle θ . Notice that the inverted pendulum system in Fig. 2 may not be in an inertia frame when the bicycle is in motion. Therefore, in addition to the gravitational force, one also has to consider the inertia force $m\frac{dv_y}{dt}$ and the centrifugal force $m\frac{v^2}{r}\cos\gamma$ acting on COG when deriving the dynamic equation. Applying Newton's law and substituting the expressions of v and v_y in (4) and (5), the lateral dynamics is derived as:

$$\begin{aligned} m\ell^2\ddot{\theta} &= m\ell\cos\theta\left(\frac{v^2}{r}\cos\gamma + \frac{dv_y}{dt}\right) + mgl\sin\theta \\ &= m\ell\cos\theta\left(\frac{v_0^2}{b}\tan\eta + \frac{av_0\sec^2\eta}{b}\dot{\eta}\right. \\ &\quad \left. + \frac{atan\eta}{b}\dot{v}_0\right) + mgl\sin\theta \end{aligned} \quad (6)$$

in which the second equality also utilizes the relation $\tan\gamma = \frac{a}{b}\tan\eta$ inferred from (2).

When both the directional angle η and the roll angle θ are small, the nonlinear dynamics in (6) can be further linearized as

$$m\ell^2\ddot{\theta} \approx m\ell\left[\left(\frac{v_0^2}{b} + \frac{av_0}{b}\right)\eta + \frac{av_0}{b}\dot{\eta}\right] + mgl\theta \quad (7)$$

It should be noted that the directional change of the front wheel is due to the vertical projection of the rotation of the steering handlebar via the caster angle of the front fork assembly (The reader can refer to (Tanaka and Murakami, 2004) for the graphical definition of the caster angle.). Denoting the steering angle of the handlebar by δ and the caster angle by ε_0 , the directional angle η can be expressed as

$$\eta = \sin\varepsilon_0 \cdot \delta. \quad (8)$$

Substituting the above expression into (7) yields

$$m\ell^2\ddot{\theta} = m\ell\frac{\sin\varepsilon_0}{b}\left[(v_0^2 + av_0)\delta + av_0\dot{\delta}\right] + mgl\theta, \quad (9)$$

or

$$\ddot{\theta} - \frac{g}{\ell}\theta = \frac{a\sin\varepsilon_0v_0}{b\ell}\left[\dot{\delta} + \left(\frac{v_0}{a} + \frac{\dot{v}_0}{v_0}\right)\delta\right] \quad (10)$$

2.3 A State-space Model for Control Design

According to (10), the open-loop system is unstable due to the inverted pendulum mode which contains an unstable pole at $\sqrt{\frac{g}{\ell}}$. As a result, feedback control is needed to modulate the steering angle to stabilize/balance the bicycle. For control design purposes, we first convert (10) into a state-space form by defining the state vector \mathbf{x} as $[\theta \quad \dot{\theta} \quad \delta]^T$ and a new control input as

$$u = \dot{\delta} + \left(\frac{v_0}{a} + \frac{\dot{v}_0}{v_0}\right)\delta, \quad (11)$$

and the state equation of the linearized lateral dynamics of the bicycle is thus given as

$$\dot{\mathbf{x}} = \mathbf{A}\mathbf{x} + \mathbf{B}u, \quad (12)$$

$$\text{where } \mathbf{A} = \begin{bmatrix} 0 & 1 & 0 \\ \frac{g}{\ell} & 0 & 0 \\ 0 & 0 & -\frac{v_0}{a} - \frac{\dot{v}_0}{v_0} \end{bmatrix}, \mathbf{B} = \begin{bmatrix} 0 \\ \frac{a\sin\varepsilon_0v_0}{b\ell} \\ 1 \end{bmatrix}.$$

The major challenge in the feedback control design is that the presence of v_0 and \dot{v}_0 in the \mathbf{A} and \mathbf{B} matrices makes the system dynamics time-varying when the bicycle experiences speed changes. To facilitate control design for the time-varying system, we assume that the bounds for v_0 and $\frac{\dot{v}_0}{v_0}$ are known, or $(v_0)_{min} \leq v_0 \leq (v_0)_{max}$ and $\left(\frac{\dot{v}_0}{v_0}\right)_{min} \leq \frac{\dot{v}_0}{v_0} \leq \left(\frac{\dot{v}_0}{v_0}\right)_{max}$ where $(v_0)_{min}$ and $(v_0)_{max}$ are respectively the lower bound and upper bound for v_0 and $\left(\frac{\dot{v}_0}{v_0}\right)_{min}$, and $\left(\frac{\dot{v}_0}{v_0}\right)_{max}$ are respectively the lower bound and upper bound for $\frac{\dot{v}_0}{v_0}$.

Next we define two parameters α and β to represent the normalized values for v_0 and $\frac{\dot{v}_0}{v_0}$ respectively as

$$\alpha = \frac{v_0 - (v_0)_{min}}{(v_0)_{max} - (v_0)_{min}}, \quad (13)$$

$$\beta = \frac{\dot{v}_0/v_0 - (\dot{v}_0/v_0)_{min}}{(\dot{v}_0/v_0)_{max} - (\dot{v}_0/v_0)_{min}} \quad (14)$$

in which $0 \leq \alpha, \beta \leq 1$. When v_0 and $\frac{\dot{v}_0}{v_0}$ in (12) are replaced by α and β respectively, it can be derived that

$$\dot{\mathbf{x}} = \mathbf{A}_0\mathbf{x} + \mathbf{B}_0u + \alpha\mathbf{A}_\alpha\mathbf{x} + \alpha\mathbf{B}_\alpha u + \beta\mathbf{A}_\beta\mathbf{x} \quad (15)$$

$$\text{where } \mathbf{A}_0 = \begin{bmatrix} 0 & 1 & 0 \\ \frac{g}{\ell} & 0 & 0 \\ 0 & 0 & -\frac{(v_0)_{min}}{a} - \left(\frac{\dot{v}_0}{v_0}\right)_{min} \end{bmatrix}, \mathbf{B}_0 = \begin{bmatrix} 0 \\ \frac{a\sin\varepsilon_0v_0}{b\ell} \\ 1 \end{bmatrix}, \mathbf{A}_\alpha = \begin{bmatrix} 0 & 0 & 0 \\ 0 & 0 & 0 \\ 0 & 0 & -\frac{(v_0)_{max} - (v_0)_{min}}{a} \end{bmatrix},$$

$$\mathbf{B}_\alpha = \begin{bmatrix} 0 \\ \frac{a\sin\varepsilon_0}{b\ell}((v_0)_{max} - (v_0)_{min}) \\ 0 \end{bmatrix}, \text{ and } \mathbf{A}_\beta = \begin{bmatrix} 0 & 0 & 0 \\ 0 & 0 & 0 \\ 0 & 0 & -((\dot{v}_0/v_0)_{max} - (\dot{v}_0/v_0)_{min}) \end{bmatrix}.$$

3 ROBUST BALANCING CONTROL DESIGN

Given the transformed dynamic model in (15), the control target is to devise a control law for u so as

to robustly regulate the state \mathbf{x} under the bounded and time-varying parameters α and β . The control problem is solved by firstly converting the model into a so-called ‘‘polytopic form’’(Zak, 2003) as

$$\dot{\mathbf{x}} = \sum_{k=1}^4 \rho_k(t) (\mathbf{A}_k \mathbf{x} + \mathbf{B}_k \mathbf{u}) \quad (16)$$

in which (15) is expressed as a linear combination of four linear systems with system matrices $\mathbf{A}_{(\cdot)}$ and $\mathbf{B}_{(\cdot)}$. The derivation of the polytopic form and the definitions of $\mathbf{A}_{(\cdot)}$, $\mathbf{B}_{(\cdot)}$, and $\rho_{(\cdot)}$ are depicted in the following lemma.

Lemma. *The dynamic model in (15) can be transformed into the polytopic form in (16) with*

$$\rho_1(t) = (1 - \alpha)(1 - \beta) \quad (17)$$

$$\rho_2(t) = \alpha(1 - \beta) \quad (18)$$

$$\rho_3(t) = (1 - \alpha)\beta \quad (19)$$

$$\rho_4(t) = \alpha\beta, \quad (20)$$

and

$$\mathbf{A}_1 = \mathbf{A}_0, \quad \mathbf{B}_1 = \mathbf{B}_0,$$

$$\mathbf{A}_2 = \mathbf{A}_0 + \mathbf{A}_\alpha, \quad \mathbf{B}_2 = \mathbf{B}_0 + \mathbf{B}_\alpha$$

$$\mathbf{A}_3 = \mathbf{A}_0 + \mathbf{A}_\beta, \quad \mathbf{B}_3 = \mathbf{B}_0$$

$$\mathbf{A}_4 = \mathbf{A}_0 + \mathbf{A}_\alpha + \mathbf{A}_\beta, \quad \mathbf{B}_4 = \mathbf{B}_0 + \mathbf{B}_\alpha.$$

Proof. Because the definitions of $\rho_{(\cdot)}$ in (17)-(20) lead to $\rho_2 + \rho_4 = \alpha$, $\rho_3 + \rho_4 = \beta$, and $\sum_{k=1}^4 \rho_k = 1$, (15) can be rewritten as

$$\begin{aligned} \dot{\mathbf{x}} &= \left(\sum_{k=1}^4 \rho_k \right) (\mathbf{A}_0 \mathbf{x} + \mathbf{B}_0 \mathbf{u}) \\ &+ (\rho_2 + \rho_4) (\mathbf{A}_\alpha \mathbf{x} + \mathbf{B}_\alpha \mathbf{u}) \\ &+ (\rho_3 + \rho_4) \mathbf{A}_\beta \mathbf{x}. \end{aligned} \quad (21)$$

By regrouping the above equation in the form of (16), one can prove that \mathbf{A}_k 's and \mathbf{B}_k 's should satisfy the expressions in the lemma. \square

Notice that the linear combination in (16) is convex that in addition to $\sum_{k=1}^4 \rho_k = 1$, the time-varying coefficients $\rho_k(t)$'s all fall between 0 and 1 due to $0 \leq \alpha, \beta \leq 1$. Models in this form are commonly referred as Takagi-Sugeno-Kang (TSK) fuzzy models. In the fuzzy control research, TSK models have been used extensively to design stabilizing controllers for nonlinear systems. In this study, we adopt a similar control structure as the fuzzy full-state feedback law(Zak, 2003) for the TSK models to stabilize the lateral dynamics of the bicycle under speed variations. The controller is a convex combination of four linear,

full-state feedback controllers with the same convex coefficients as the plant model in (16):

$$\mathbf{u} = \sum_{j=1}^4 \rho_j \mathbf{K}_j \mathbf{x}, \quad (22)$$

where \mathbf{K}_j 's are feedback gain matrices. The associated closed-loop dynamics is given by

$$\dot{\mathbf{x}} = \sum_{k=1}^4 \sum_{j=1}^4 \rho_k \rho_j (\mathbf{A}_k + \mathbf{B}_k \mathbf{K}_j) \mathbf{x} \quad (23)$$

The following theorem provides a synthesis method for computing the stabilizing gain matrices \mathbf{K}_j 's.

Theorem. *Given the polytopic system in (16) with the control law in (22), for $\mathbf{W} = \mathbf{W}^T > \mathbf{0} \in \mathbb{R}^{4 \times 4}$ and $\lambda > 0 \in \mathbb{R}$, if there exist $\mathbf{Y}_1, \mathbf{Y}_2, \mathbf{Y}_3, \mathbf{Y}_4 \in \mathbb{R}^{2 \times 4}$ satisfying the following linear matrix inequalities (LMI's):*

$$\begin{aligned} (\mathbf{A}_k + \mathbf{A}_j) \mathbf{W} + \mathbf{W} (\mathbf{A}_k + \mathbf{A}_j)^T + (\mathbf{Y}_j^T \mathbf{B}_k^T \\ + \mathbf{B}_k \mathbf{Y}_j) + (\mathbf{Y}_k^T \mathbf{B}_j^T + \mathbf{B}_j \mathbf{Y}_k) + 4\lambda \mathbf{W} \leq \mathbf{0} \end{aligned} \quad (24)$$

for all $k \leq j$, $k, j \in \{1, 2, 3, 4\}$, then the closed-loop system is globally exponentially stable by setting

$$\mathbf{K}_j = \mathbf{Y}_j \mathbf{W}^{-1}, j = 1 \sim 4. \quad (25)$$

Furthermore, $\|\mathbf{x}(t)\|_2$ is bounded by $C \|\mathbf{x}(0)\|_2 e^{-\lambda t}$ for some finite constant C .

Proof. For the Lyapunov function defined by $V(\mathbf{x}) = \frac{1}{2} \mathbf{x}^T \mathbf{P} \mathbf{x}$ where $\mathbf{P} = \mathbf{W}^{-1}$, its time derivative along the closed-loop system trajectory (23) is

$$\begin{aligned} \dot{V} &= \sum_{k=1}^4 \sum_{j=1}^4 \rho_k \rho_j \mathbf{x}^T [\mathbf{P} (\mathbf{A}_k + \mathbf{B}_k \mathbf{K}_j) \\ &+ (\mathbf{A}_k^T + \mathbf{K}_j^T \mathbf{B}_k^T) \mathbf{P}] \mathbf{x}. \end{aligned} \quad (26)$$

Substituting the gain matrices of (25) into \dot{V} yields

$$\begin{aligned} \dot{V}(\mathbf{x}) &= \sum_{k=1}^4 \sum_{j=1}^4 \rho_k \rho_j \mathbf{x}^T \mathbf{P} [(\mathbf{A}_k \mathbf{W} + \mathbf{B}_k \mathbf{Y}_j) \\ &+ (\mathbf{W} \mathbf{A}_k^T + \mathbf{Y}_j^T \mathbf{B}_k^T)] \mathbf{P} \mathbf{x} \end{aligned} \quad (27)$$

The terms in \dot{V} is further regrouped as

$$\begin{aligned} \dot{V} &= \sum_{k=1}^4 \rho_k^2 \mathbf{x}^T \mathbf{P} [(\mathbf{A}_k \mathbf{W} + \mathbf{B}_k \mathbf{Y}_k) \\ &+ (\mathbf{W} \mathbf{A}_k^T + \mathbf{Y}_k^T \mathbf{B}_k^T)] \mathbf{P} \mathbf{x} + \sum_{k=1}^4 \sum_{j>k}^4 \rho_k \rho_j \mathbf{x}^T \cdot \\ &\mathbf{P} [(\mathbf{A}_k + \mathbf{A}_j) \mathbf{W} + \mathbf{W} (\mathbf{A}_k + \mathbf{A}_j)^T + \\ &(\mathbf{Y}_j^T \mathbf{B}_k^T + \mathbf{B}_k \mathbf{Y}_j) + (\mathbf{Y}_k^T \mathbf{B}_j^T + \mathbf{B}_j \mathbf{Y}_k)] \mathbf{P} \mathbf{x} \end{aligned} \quad (28)$$

By applying (24) with $j = k$ to the terms associated with $\sum \alpha_k^2$ and with $j > k$ to the terms associated with $\sum \rho_k \rho_j$, and using the relations that $0 \leq \rho_{(\cdot)} \leq 1$ and $\mathbf{P}\mathbf{W} = \mathbf{I}$, it can be derived that \dot{V} in (28) is upper bounded by:

$$\begin{aligned} \dot{V} &\leq -2\lambda \sum_{k=1}^4 \rho_k^2 \mathbf{x}^T \mathbf{P} \mathbf{x} - 4\lambda \sum_{k=1}^4 \sum_{j>k}^4 \rho_k \rho_j \mathbf{x}^T \mathbf{P} \mathbf{x} \\ &\leq -2\lambda \left(\sum_{k=1}^4 \rho_k \right)^2 \mathbf{x}^T \mathbf{P} \mathbf{x} = -2\lambda \mathbf{x}^T \mathbf{P} \mathbf{x} \quad (29) \end{aligned}$$

in which the last equality is due to $\sum \rho_k = 1$. Therefore, \dot{V} is negative-definite and the asymptotic stability of the closed-loop system is proved. The exponential stability follows from $\dot{V} \leq -2\lambda V$ (Slotine and Li, 1991). \square

4 SIMULATION STUDIES

Although the proposed balancing controller is designed based on the linearized model, for numerical verifications, it is applied to the nonlinear model in (6) to simulate the control performance. The system parameters used are listed in Table 1.

Table 1: Parameters of the bicycle model used in the simulations.

a	0.3957 m	m	23.1 kg
b	1.053 m	ℓ	0.4338 m
ε_0	20°		

The controller design assumes that $(v_0)_{min} = 1.5m/s$, $(v_0)_{max} = 10m/s$, $\left(\frac{\dot{v}_0}{v_0}\right)_{min} = -2.5/s$ and $\left(\frac{\dot{v}_0}{v_0}\right)_{max} = 4/s$. The four full-state feedback gain matrices computed by LMI's are $\mathbf{K}_1 = [-185.12, -71.10, 0.40]$, $\mathbf{K}_2 = [-713.31, -273.49, 22.39]$, $\mathbf{K}_3 = [-693.76, -266.32, 16.68]$, and $\mathbf{K}_4 = [-801.19, -307.05, 26.76]$. In the first simulation, we examine the stabilization properties of the proposed controller under speed variations. It is desired that the closed-loop system is stabilized around the equilibrium point $\mathbf{x} = \mathbf{0}$ which means that steering the bicycle in a straight manner is of interests. The initial state is set as $\mathbf{x}(0) = [5^\circ \ 0^\circ/s \ 0^\circ]^T$. Fig. 3 displays the responses of θ , $\dot{\theta}$, and δ of the proposed controller as well as the speed history used in the simulation. One can see that as the bicycle accelerates linearly from $1.5m/s$ to $10m/s$, the controller is capable of centering the bicycle and

maintain the lateral stability. The maximum steering angle is kept within 15° . The second simulation is to

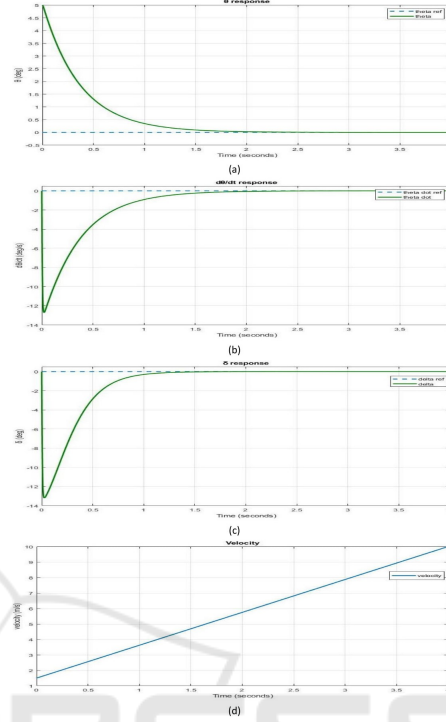


Figure 3: Simulated straight-line steering responses for the proposed controller.

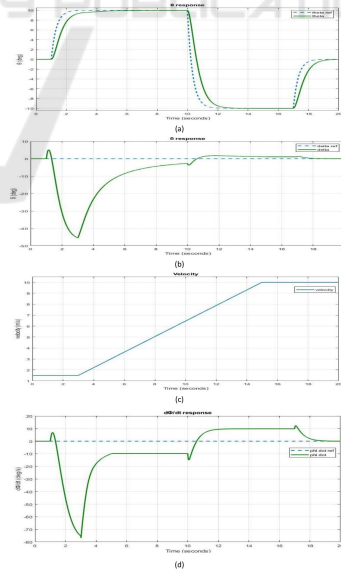


Figure 4: Simulated cornering responses for the proposed controller.

examine the cornering performance of the proposed controller. Cornering of the bicycle is achieved by imposing a nonzero roll angle command θ_d which



Figure 5: Photo of the prototype bicycle.

is generated as a filtered $\pm 10^\circ$ square wave. The simulated responses for the roll angle, steering angle, velocity, and yaw rate are shown in Fig. 4. The proposed controller is able to make the roll angle track the desired command under speed variations. The tracking of the roll angle command generates corresponding steering angle response, which by (3) and (8), causes the yaw rate response so that the bicycle first turns right and then turns left. Notice that the steering angle response exhibits undershoot during cornering. Such a phenomenon, which matches the experience of cornering an actual bicycle, is a typical non-minimum-phase behavior due to the unstable open-loop dynamics in (10).

5 EXPERIMENTAL VERIFICATIONS

A prototype bicycle is constructed for experimental validation. The bicycle contains a 500W brushless DC wheel motor as the rear wheel. The motor speed is regulated by a motor control unit which contains a motor driver and an STM32F401RE MCU board. A servo motor is installed on the pivot of the handlebar to provide steering action. An inertial measurement unit (IMU) which contains a three-axis accelerometer and a three-axis gyro is attached to the bicycle frame. The sensor fusion algorithm developed previously by the authors (Huang et al., 2018), which not only considers the multi-axis coupling among the sensor signals but also accounts for the dynamic effects including the longitudinal acceleration and centrifugal acceleration, is adopted to compute roll angle, roll rate and yaw rate of the bicycle. Both the sensor fusion and the control algorithm are implemented on another STM32F401RE MCU board. To provide support at stationary position and low speeds, the bicycle

is also equipped with a set of landing gears which can be actuated by linear electric actuators. The photo of the prototype bicycle is shown in Fig. 5.

Experiments are conducted to compare the balancing performances of the proposed controller designed as in the simulation section and a fixed-gain, full-state feedback controller designed using LQR approach under constant speed assumption. First we consider steering the bicycle in straight line. The responses in Fig. 6 indicate that the fixed-gain LQR controller is unable to cope with speed changes that the roll angle and steering angle start to diverge at about 3s which eventually leads to bicycle fall. Fig. 7 shows the responses of the proposed controller. The controller is able to maintain the lateral balance by keeping the roll angle within 3° . Notice that during the experiment, the bicycle was supported by the landing gears initially and at low speeds. Once the speed reaches $0.5m/s$, the land gears are lifted automatically by the linear actuators and the bicycle is balanced autonomously. The cornering performance of the proposed controller is also examined experimentally. A filtered square wave command for the roll angle is adopted. According to the responses in Fig. 8, the roll angle can basically follow the reference command.

6 CONCLUSIONS

This paper is devoted to the balancing control of a self-driving bicycle. The proposed controller is a convex combination of four linear, full-state feedback controllers, which is specifically designed to cope with the convex structure in the bicycle's lateral dynamics under speed variations. The stability of the control system is theoretically proved and a systematic procedure to compute the control gain matrices is given. Both simulations and experiments verify that the proposed controller can provide robust balancing performance under various operating conditions. Ongoing research efforts include incorporating cameras, GPS sensors and so on to study collision avoidance and autonomous navigation of the self-driving bicycle.

ACKNOWLEDGMENT

The authors gratefully acknowledge the support provided by Ministry of Science and Technology in Taiwan.

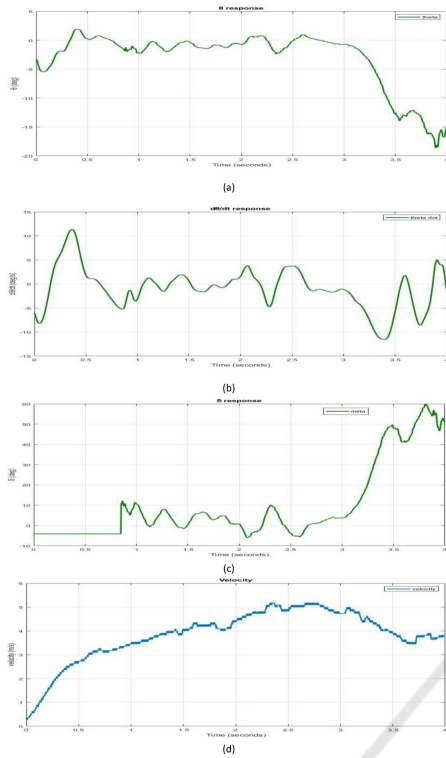


Figure 6: Experimental straight-line steering responses under LQR control.

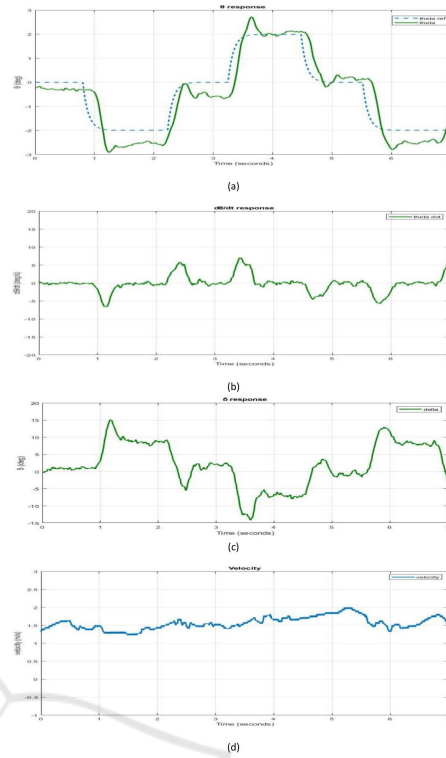


Figure 8: Experimental cornering responses under the proposed controller.

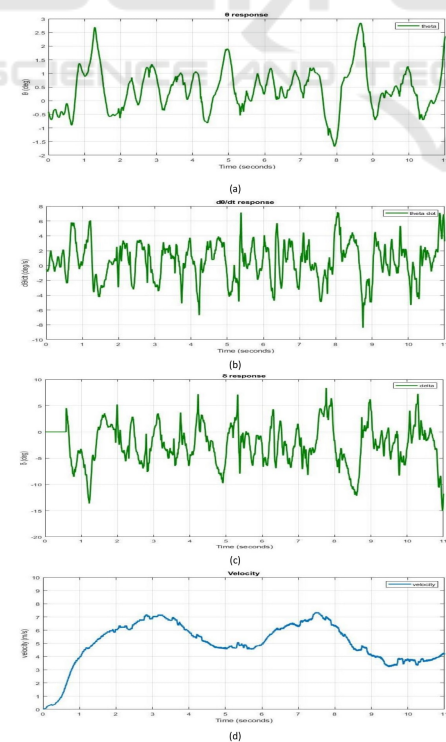


Figure 7: Experimental straight-line steering responses under the proposed controller.

REFERENCES

Astrom, K. J., Klein, R. E., and Lennartsson, A. (2005). Bicycle dynamics and control: adapted bicycles for education and research. *IEEE Control Systems*, 25(4):26–47.

Beznos, A. V., Formal'sky, A. M., Gurfinkel, E. V., Jicharev, D. N., Lensky, A. V., Savitsky, K. V., and Tchetalin, L. S. (1998). Control of autonomous motion of two-wheel bicycle with gyroscopic stabilisation. In *Robotics and Automation, 1998. Proceedings. 1998 IEEE International Conference on*, volume 3, pages 2670–2675 vol.3.

Cerone, V., Andreo, D., Larsson, M., and Regruto, D. (2010). Stabilization of a riderless bicycle: A linear-parameter-varying approach. In *IEEE Control Syst. Mag.* Citeseer.

Huang, C.-F., Dai, B.-H., and Yeh, T.-J. (2018). Determination of motor torque for power-assist electric bicycles using observer-based sensor fusion. *Journal of Dynamic Systems, Measurement, and Control*, 140(7):071019.

Huang, C. F., Tung, Y. C., and Yeh, T. J. (2017). Balancing control of a robot bicycle with uncertain center of gravity. In *2017 IEEE International Conference on Robotics and Automation (ICRA)*, pages 5858–5863.

Lowell, J. and McKel, H. D. (1982). The stability of bicycles. *American Journal of Physics*, 50:1106–1112.

- Meijaard, J. P., Papadopoulos, J. M., Ruina, A., and Schwab, A. L. (2007). Linearized dynamics equations for the balance and steer of a bicycle: a benchmark and review. In *Proceedings of the Royal Society of London A: Mathematical, Physical and Engineering Sciences*, volume 463, pages 1955–1982. The Royal Society.
- Sharp, R. S. (1971). The stability and control of motorcycles. *Journal of mechanical engineering science*, 13(5):316–329.
- Slotine, J.-J. E. and Li, W. (1991). *Applied nonlinear control*, volume 199. Prentice hall Englewood Cliffs, NJ.
- Tanaka, Y. and Murakami, T. (2004). Self sustaining bicycle robot with steering controller. In *Advanced Motion Control, 2004. AMC '04. The 8th IEEE International Workshop on*, pages 193–197.
- Whipple, F. J. (1899). The stability of motion of a bicycle. *Quarterly Journal of Pure and Applied Mathematics*, 30:312–348.
- Zak, S. H. (2003). *Systems and control*, volume 174. Oxford University Press New York.

